Available online at www.sciencedirect.com

SCIENCE DIRECT

Brain Research 1040 (2005) 14–28

BRAIN RESEARCH

www.elsevier.com/locate/brainres

Research report

Evidence that urocortin I acts as a neurohormone to stimulate αMSH release in the toad *Xenopus laevis*

Marinella Calle[a,b,*], Geert J.H. Corstens[a], Liangchun Wang[a], Tamas Kozicz[a], Robert J. Denver[c], Henk P. Barendregt[b], Eric W. Roubos[a]

[a]*Department of Cellular Animal Physiology, Radboud University Nijmegen, Nijmegen, The Netherlands*
[b]*Department of Computer Science, Radboud University Nijmegen, Nijmegen, The Netherlands*
[c]*Department of Molecular, Cellular and Developmental Biology, University of Michigan, Ann Arbor, MI 48109, USA*

Accepted 17 December 2004
Available online 17 March 2005

Abstract

We have raised the hypothesis that in the South African clawed toad *Xenopus laevis*, urocortin 1 (UCN1), a member of the corticotropin-releasing factor (CRF) peptide family, functions not only within the brain as a neurotransmitter/neuromodulator but also as a neurohormone, promoting the release of α-melanophore-stimulating hormone (αMSH) from the neuroendocrine melanotrope cells in the intermediate lobe of the pituitary gland. This hypothesis has been investigated by (1) assessing the distribution of UCN1 and CRF by light immunocytochemistry, (2) determining the subcellular presence of UCN1 in the neural lobe of the pituitary gland by immuno-electron microscopy applying high-pressure freezing and cryosubstitution, and (3) testing the effect of UCN1 on MSH release from toad melanotrope cells using in vitro superfusion.

In the *X. laevis* brain, the main site of UCN1-positive somata was found to be the Edinger–Westphal nucleus. UCN1 immunoreactivity (ir) also occurs in the nucleus posteroventralis tegmenti, central gray, nucleus reticularis medius, nucleus motorius nervi facialis, and nucleus motorius nervi vagi. UCN1 occurs together with CRF in the nucleus motorius nervi trigemini, and in the magnocellular nucleus, which send a UCN1- and CRF-containing fiber tract to the median eminence. Strong UCN1-ir and CRF-ir were found in the external zone of the median eminence. From the internal zone of the median eminence, UCN1-ir fibers, but few CRF-ir fibers, were found to project to the pituitary neural lobe, where they form numerous neurohemal axon terminals. Ultrastructurally, two types of terminal containing UCN1-ir secretory granules were distinguished: type A contains large, moderately electron-dense, round secretory granules and type B is filled with smaller, strongly electron-dense, ellipsoid secretory granules. In vitro superfusion studies showed that UCN1 stimulated the release of αMSH from melanotrope cells in a dose-dependent manner.

Our results support the hypothesis that in *X. laevis*, UCN1 released from neurohemal axon terminals in the pituitary neural lobe functions as a stimulatory neurohormone for αMSH release from melanotrope cells of the pituitary intermediate lobe.

Theme: Endocrine and autonomic regulation
Topic: Neuroendocrine regulation: other

Keywords: Neural pituitary lobe; Corticotropin-releasing factor; Melanotrope cells; Magnocellular nucleus; High-pressure freezing; Cryosubstitution; Immuno-electron microscopy

1. Introduction

Urocortin I (UCN1) is a 40 amino acid peptide first isolated from rat brain by molecular cloning in 1995 [44]. It is a member of the corticotropin-releasing factor (CRF) peptide family and exhibits 45% amino acid sequence

* Corresponding author. Department of Cellular Animal Physiology, Institute for Neuroscience, Radboud University Nijmegen, Nijmegen, The Netherlands. Fax: +31 24 365 2714.
E-mail address: m.calle@science.ru.nl (M. Calle).

0006-8993/$ - see front matter © 2005 Elsevier B.V. All rights reserved.
doi:10.1016/j.brainres.2004.12.056

similarity to rat CRF, 63% sequence similarity to carp urotensin I and 35% sequence similarity to sauvagine [44]. The main sites of UCN1 production in the mammalian brain are the Edinger–Westphal nucleus, from which UCN1 is transported to the spinal cord, the lateral septum [2,33], and the lateral superior olive where UCN1 is proposed to target accessory optic, precerebellar and auditory structures, and the spinal intermediate gray. In addition, moderate levels of UCN1-immunoreactivity (ir) occur in the cerebellum, hippocampus, neocortex, olfactory system, basal ganglia, amygdala, and the supraoptic, ventromedial, and paraventricular nuclei of the hypothalamus [2,17,22]. In amphibians, UCN1-ir was reported in the brain of the frog *Rana esculenta*, where it mainly occurs in the Edinger–Westphal nucleus, anterior preoptic area, ventromedial thalamic nucleus, nucleus of the posterior tuberculum, and the nucleus of the medial longitudinal fasciculus [18].

UCN1 may have a diversity of functions. It clearly has anorectic activity, inhibiting food intake via the ventromedial hypothalamic nucleus and the hypothalamic paraventricular nucleus [23,48]. A role for UCN1 in stress adaptation is suggested by the fact that it may be released from the rat Edinger–Westphal nucleus under conditions of chronic stress [16] and is down-regulated in the Edinger–Westphal nucleus in mice over-expressing CRF [19]. While UCN1 in the brain probably acts on central neurons in both synaptic and non-synaptic ("volume transmission") ways, there is circumstantial evidence that UCN1 can also control peripheral targets. In the rat, UCN1 increases heart rate, probably via its action on CRF type 2 receptors (CRF_2) [4,26] and may induce a drop in blood pressure via mesenteric vasodilatation [26]. Moreover, the stimulatory action of UCN1 on ACTH release from the distal lobe of the rat pituitary gland suggests that UCN1 can act as a neurohormone [1]. However, the sites of synthesis and release of corticotrope-stimulating UCN1 are unknown.

In the present study, we analyzed the distribution and possible neurohormonal actions of UCN1 in the South African clawed toad, *Xenopus laevis.* This species was chosen because it is a well-established model for studying the functioning and regulation of the intermediate lobe of the pituitary gland [14,15,27–30,37,38,45] but the roles of CRF and UCN in these processes are unclear. The neurohormonal and neural control of the release of α-melanophore-stimulating hormone (αMSH) from the melanotrope cells of the *Xenopus* intermediate pituitary lobe has been extensively studied. A rise in circulating αMSH causes darkening of the animal's skin, a process known to occur in response to environmental challenges like placing the animal on a dark background or lowering the ambient water temperature [27–30,37,38]. Various inhibitory and stimulatory factors are proposed to control the release of αMSH from the melanotrope cells, including CRF [14,15,45]. Because both the *X. laevis* magnocellular nucleus and the neural lobe of the pituitary gland stained positively with an antiserum raised against mammalian CRF [45], it has been proposed that CRF is released from neurohemal axon terminals in the neural lobe and diffuses towards the pars intermedia to activate the melanotropes [14]. However, CRF-immunopositivity was also seen in the median eminence [45], leaving open the possibility that it acts on the melanotropes via the classical median eminence–pituitary portal system.

The homology of xCRF with both rat and human CRF is 93% [34] and the homologies of xUCN1 with rat and human UCN1 are 70% and 65%, respectively [8,53]. Recently, Dautzenberg and colleagues [5–7] isolated cDNAs for two *X. laevis* CRF receptors, $xCRF_1$ and $xCRF_2$, which share a high degree of sequence similarity with their mammalian counterparts. We recently demonstrated by RT-PCR the expression of both $xCRF_1$ and $xCRF_2$ mRNAs in the *X. laevis* neurointermediate lobe (B.G. Jenks, unpublished results). The $xCRF_1$ binds xCRF with higher affinity than *X. laevis* UCN1, but the $xCRF_2$ binds both peptides with similar high affinity (G.C. Boorse and R.J. Denver, unpublished results). Based on these results, we have raised the hypothesis that in *X. laevis* both CRF and UCN1 function as neurohormones controlling the pituitary melanotrope cells.

We have tested this hypothesis by analyzing the distribution of UCN1-ir in comparison to that of CRF-ir in the brain and pituitary gland of *X. laevis*. We paid special attention to potential sites where these peptides could be released to act on the melanotrope cells, viz., the median eminence of the hypothalamus and, in particular, the neural lobe of the pituitary gland. Affinity-purified antibodies were used that had been generated against synthetic xCRF to detect xCRF-ir. To detect UCN1-ir in *X. laevis*, we used an antiserum to rat UCN1, and verified the specificity of the immunoreaction by preabsorption with synthetic *X. laevis* peptides. We also determined the subcellular distribution of UCN1 in the pituitary neural lobe by immuno-electron microscopy, applying our recently developed high-pressure freezing (HPF) and cryosubstitution method [49]. Finally, the effect of UCN1 on αMSH release from *X. laevis* melanotrope cells was tested in an in vitro superfusion study.

2. Methods

2.1. Animals

Forty adult (6 months) specimens of *X. laevis*, with a body weight of 28–32 g, were raised under standard laboratory conditions and fed weekly on ground beef heart and Trouvit trout pellets (Trouw, Putten, The Netherlands). They were kept under constant illumination at a water temperature of 22 ± 1 °C, and adapted to a gray background for 3 weeks. All experiments were carried out under the guidelines of the Dutch law concerning animal welfare.

2.2. Tissue preparation for light microscopic immunocytochemistry

Twenty-five toads were deeply anaesthetized by immersion in a solution of 0.1% tricaine methane sulfonate (MS222; Novartis, Basel, Switzerland) in tap water transcardially perfused with ice-cold 0.6% sodium chloride, for 5 min, and perfused with 250 ml ice-cold Bouin's fixative, for 15 min. After decapitation, brain and pituitary gland, either attached to it or separated, were dissected and postfixed in the same fixative, for 16 h at 4 °C, and washed in 70% ethanol, to eliminate excess of picric acid, for 24 h, and dehydrated in a graded ethanol series.

2.3. Free-floating immunocytochemistry

Fifteen fixed brains without the pituitary glands were embedded in gelatine and 40-μm serial coronal sections were cut with a Leica vibratome (Leica, Wetzlar, Germany). After four 15-min washes in sodium phosphate-buffered saline (PBS; pH 7.4), sections were treated with 0.3% hydrogen peroxide (H_2O_2) for 30 min to inactivate endogenous peroxidase. After two 15-min washes in PBS, sections were incubated in 0.5% Triton X-100 (Sigma, St. Louis, MO, USA) for 30 min, to enhance antibody penetration. After an additional four 15-min washes in PBS, sections were incubated in 2% normal goat serum (NGS) in PBS for 1 h. All steps were carried out at 20 °C, under continuous, gentle agitation. After a brief wash in PBS, sections were transferred to vials containing the primary antiserum.

The anti-UCN1 serum had been generated in rabbits against rat UCN1 coupled by glutaraldehyde to human α-globulin, and the high specificity of the antiserum has been demonstrated [2,40]. We previously raised in rabbit an antiserum against *X. laevis* CRF (xCRF; 3) conjugated to human α-globulin. The IgG fraction of the serum was isolated on a protein A column, and passed over an Affigel 10 affinity column to which xCRF had been coupled. Then, the IgGs were eluted from the column. The high specificity of the xCRF antiserum was shown before [3,52].

Sections of the brain and pituitary gland were incubated in primary antiserum (dilutions with 2% NGS in PBS: UCN1, 1:30,000; xCRF, 1:15), for 16 h at 20 °C, followed by four 15-min washes in PBS. For detection of immunoreactivity, an ABC elite kit (rabbit) (Vector Laboratories, Burlingame, CA, USA) was used. Immunostaining was visualized with 0.03% 3-3′-diaminobenzidine (DAB; Sigma) and 0.01% H_2O_2, in Tris–HCl, for approximately 10 min. The reaction was controlled under a microscope and was stopped by several rinses in Tris–HCl buffer. Intensification of the staining was achieved with 0.5% nickel-ammonium sulphate in the DAB solution. Then sections were rinsed once in PBS, dehydrated in a graded series of ethanol, cleared in xylene, and mounted with Entellan (Merck, Darmstadt, Germany) on gelatine-coated glass slides.

2.4. Paraffin immunocytochemistry

Ten Bouin-fixed brains with the pituitary glands attached were dehydrated through a graded series of ethanol and embedded in paraffin. Coronal sections (7 μm) were mounted on poly-L-lysine-coated slides and allowed to air-dry, for 16 h at 45 °C, deparaffinated and rehydrated. The subsequent staining procedure was carried out at 20 °C. Endogenous peroxidase activity was quenched with 0.1% H_2O_2 in PBS, for 30 min, by rinsing twice for 15 min. Then, to prevent non-specific binding, sections were rinsed for 1 h in PBS containing 0.5% Triton X-100 (PBST; Sigma) and a combination of 2.5% NGS and 2.5% normal horse serum (Vector laboratories). Sections were then rinsed in avidin/biotin blocking solution (Vector Laboratories) for 15 min, and incubated in PBST with anti-UCN1 (1:30,000) or anti-xCRF (1:15), for 16 h at 22 °C. Immunodetection was carried out with a Vectastain ABC elite kit (Vector Laboratories). After rinsing the sections in PBS and in Tris–HCl buffer for 30 min, the reaction product was visualized with 0.04% DAB (Sigma) and 0.015% H_2O_2 in Tris–HCl buffer. Intensification of the staining was achieved with 0.5% nickel-ammonium sulphate added to the DAB solution. The reaction was terminated by several rinses in Tris–HCl buffer. Finally, sections were dehydrated in a graded series of ethanol, cleared in xylene, and mounted in Entellan (Merck, Hohenbrunn, Germany).

2.5. High-pressure freezing and cryosubstitution

Five toads were decapitated and their neurointermediate pituitary lobe was dissected, rinsed in PBS, and mounted under 1-hexadecene (Merck) in the cavity of an aluminum planchette (ALU ∅ 3 × 0.5 mm and an inner cavity of ∅ 2 × 0.15 mm; Waldner, Uetliburg, Switzerland) for high-pressure freezing (HPF). The planchette was covered with the flat side of another planchette coated with lecithin (3-sn-phosphatidyl choline; Fluka, Buchs, Switzerland) to ease opening of the planchette sandwich. The sandwich was placed into a Leica HPF apparatus (Leica Microsystem, Vienna, Austria) in which the tissue was rapidly cryofixed at 2100 bar [49]. Under liquid nitrogen, the planchette sandwiches were opened and the 1-hexadecene was removed with forceps and a dissection needle. Then the frozen lobes were put into Saf-T-Seal microtubes (Biozym, Landgraaf, The Netherlands) containing 0.5% uranyl acetate and 0.2% glutaraldehyde in methanol, and kept at −90 °C in a CS Auto cryosubstitution unit (Leica). Next, a substitution program was performed: after 50 h at −90 °C, the temperature was raised in steps of 4 °C/h and maintained at −40 °C for 6 h. Then samples were washed with precooled methanol and embedded at −40 °C into Lowicryl HM20 resin (Electron Microscopy Science, Fort Washington, PA, USA). Polymerization of the resin was performed under UV irradiation at −40 °C for 16 h and at 20 °C for another 24 h [49].

2.6. Immuno-electron microscopy

For immunogold labeling, the procedure of Wang et al. [49] was followed. Ultrathin pale-gold sections from the neurointermediate pituitary lobe were collected on 250-mesh, uncoated nickel grids and incubated in PBS, for 2 × 5 min. Non-specific protein binding sites were blocked by incubation in PBS-G (0.5% bovine serum albumin, fraction V, and 0.045% teleostean gelatine, both from Sigma, in PBS), for 2 × 15 min. Then, the sections were incubated with UCN1-antiserum (1:10,000) or xCRF antiserum (1:20) in PBS-G, for 16 h. After washing in PBG for 6 × 5 min, sections were incubated with 10 nm gold-conjugated secondary goat-anti-rabbit serum (BB International, Cardiff, UK) in a dilution of 1:50, for 2 h. Then they were washed with PBG and PBS, each for 4 × 5 min, postfixed in 1% glutaraldehyde in PBS for 15 min, and contrasted with uranyl acetate and lead citrate. Sections were examined with a Jeol 1010 electron microscope (Jeol, Tokio, Japan).

2.7. Immunocytochemistry controls

The specificities of the antisera were confirmed by preabsorption with synthetic peptides (50 μg/ml) for 16 h at 4 °C, before immunocytochemistry. The *X. laevis* UCN1 and UCN3 peptides were synthesized by the protein structure facility at the University of Michigan based on the deduced amino acid sequences (Genbank accession #AY596827 and #AY596826, respectively; G.C. Boorse and R.J. Denver, unpublished results). Both peptides were synthesized on an Applied Biosystems 433A peptide synthesizer using FMOC solid phase peptide chemistry and purified by reversed phase-HPLC to greater than 90% purity. Preabsorption of the anti-xCRF serum with xCRF abolished the immunoreaction whereas, preabsorption with UCN1 or UCN3 and the structurally related peptide sauvagine (Bachem, Bubendorf, Switzerland) had no effect (see also [52]). Preabsorption of the anti-UCN1 serum with *X. laevis* UCN1 abolished staining, while CRF (rat; see also [18]) or *X. laevis* UCN3 and sauvagine (see also [18]) had no effect.

2.8. Superfusion

Six animals were decapitated, their neurointermediate pituitary lobes dissected, and melanotrope cells isolated as described before [31]. In short, lobes were incubated for 45 min in Ringer's solution without $CaCl_2$ to which 0.25% (w/v) trypsin (Gibco, Renfrewshore, UK) had been added. Cells were subsequently dispersed in Leibovitz's L15 medium (Life Technologies, Paisley, UK) adjusted to *X. laevis* blood osmolality (XL15; L15: ultrapure water = 2:1) and containing 10% fetal calf serum (Gibco), by gentle trituration of the lobes with a siliconized Pasteur's pipette. After washing, cells were resuspended in lysine-free XL15 and in dialyzed fetal calf serum (FCS; Life Technologies). After centrifugation, cells were resuspended in lysine-free XL15 containing 250 μCi ^{3}H-labeled lysine (Amersham, Buckinghamshire, UK) and plated onto poly-L-lysine-coated 15 mm ∅ glass cover slips. After the cells had been allowed to attach for 1 h, they were cultured for 2 days at 22 °C in humidified atmosphere in lysine-free XL15 containing 10% dialyzed FCS. For superfusion, cells were rinsed with *X. laevis* Ringer's four times and placed in a 4-well plate (Nuclon, Roskilde, Denmark). This was followed by superfusing the cells with Ringer's at a rate of 75 μl/min for 1.5 h, after which *X. laevis* UCN1 was added in pulses of 10 min, in different concentrations. (For protocol, see Results). Fractions were collected every 2 min and 160 μl scintillation fluid (Optiphase Supermix, Wallac, Loughborough, UK) was added. The amount of radiolabeled peptides in each fraction was determined with a scintillation counter (Wallac) and data were collected with Microbeta software (Wallac). For each experiment, the average of the first 20 fraction measurements was considered as the control release level and set as 100%. It was previously shown that about 30–50% of the radioactivity in the superfusate is unincorporated (^{3}H)lysine [31].

3. Results

3.1. Distribution of CRF and UCN1 in the X. laevis brain and pituitary gland

Light microscopic immunocytochemistry was carried out on free-floating and on paraffin sections. All data presented are essentially the same for both types of technique. However, the free-floating technique yielded a more intense immunostaining and the 40-μm-thick sections permitted us to study the course of stained fibers over relatively long distances, whereas in the 7-μm paraffin sections, individual neuronal cell bodies and thin fiber tracts could be identified more accurately. The occurrence of immunoreactive cell bodies in a brain structure was assessed in serial sections and semiquantitatively expressed as follows: 1–4: 'rare' or 'few', 5–8: 'some', 8–20: 'many' or 'numerous'. All neuronal elements described were strongly immunopositive, unless stated otherwise. The results are summarized in Table 1 and Fig. 1.

3.1.1. CRF

3.1.1.1. Telencephalon. A few round, small cell bodies (ca. 10 μm in diameter) occur in the internal granule cell layer of the olfactory bulb, surrounded by fibers. In the mitral cell layer, some cells are present together with rarely occurring fibers (Fig. 2a). Round, small cell bodies, exhibiting a rather weak staining, with moderately stained dendrites were observed in low numbers in the

Table 1
Semiquantitative distribution of CRH- and UCN1-immunoreactive cell bodies and fibers in the *X. laevis* brain and pituitary gland, as visualized by free-floating and paraffin immunocytochemistry of sections made at the levels A–Q as indicated in Fig. 1

Brain region	CRF		UCN1	
	Cells	Fibers	Cells	Fibers
Telencephalon				
Olfactory bulb, mitral cells (ml)	++	+		
Olfactory bulb, internal granule cells (igl)	+	+		+
Medial olfactory tract (mot)				+
Post-olfactory eminence (pe)	++			
Medial septum (ms)		+		+
Lateral septum (ls)	+	+		
Medial pallium (mp)		+		
Dorsal pallium (dp)		+		+
Striatum (Str)	+			+
Accumbens (Acc)	+++	+		+
Diagonal band of Broca (DB)		+		+
Amygdala pars medialis (Apm)	+	+		
Amygdala pars lateralis (Apl)	++	+		
Anterior commissure (ac)		+		
Diencephalon				
Nucleus habenularis ventralis (Hv)	+++			
Ventromedial thalamic nucleus (VM)	+			
Anterior thalamic nucleus (A)	+			+
Central thalamic nucleus (C)				+
Posterior thalamic nucleus (P)				+
Magnocellular nucleus, medial part (Mgm)	++	+	++	+
Magnocellular nucleus, ventral part (Mgv)	++	+	+++	+
Suprachiasmatic nucleus (SC)	+			
Paraventricular organ (NPv)	++	+		
Posterior tubercle (TP)	+	+		+
Ventral hypothalamic nucleus (VH)	+	+		
Median eminence zona interna		+		+
Median eminence zona externa		+		+
Pituitary pars nervosa (pn)		+		+
Mesencephalon				
Tectum mesencephali (tect)	+++	+		+
Tegmentum mesencephali (tegm)		+		+
Edinger–Westphal nucleus (E–WN)		+	+++	+
Anterior tegmental nucleus (Av, Ad)	++	+		
Posterior commissure (pc)		+		
Nucleus posteroventralis tegmenti (Pv)	+		++	
Torus semicircularis (Tor)		+		+
Rhombencephalon				
Locus coeruleus (Lc)	++	+		
Central gray (cg)			++	
Nucleus reticularis medius (Rm)			+	
Cochlear nucleus (LL)				+
Nucleus motorius nervi trigemini (Vm)	++	+	++	
Nucleus motorius of the facial and gp nerve (IX)			++	+
Nucleus motorius nervi vagi (Xm)			++	
Cerebellum (Cb)		+		

The numbers of positive cell bodies are expressed as follows: 1–4: + 'rare' or 'few'; 5–8: ++ 'some'; 8–20: +++ 'many' or 'numerous'. Immunoreactive fibers are indicated with +.

post-olfactory eminence (Fig. 2b). In the medial and dorsal pallium, many varicose fibers are present. The lateral septum reveals rare, small, fusiform but clearly immunopositive cell bodies as well as heavily stained varicose fibers, while in the medial septum, only varicose fibers appear. In the striatum, a few cell bodies were encountered. They are small and have an oval shape. Their very long dendritic processes run in both ventral and dorsal directions. In the diagonal band of Broca, many fibers occur. The nucleus accumbens contains numerous small, ovoid cell bodies with primary and secondary dendrites running ventrally, and also a few varicose fibers are present (Fig. 2c, inset). In the medial part of the amygdala sparsely occurring, round cell bodies were seen, whereas in the lateral part of the amygdala, some cell bodies with an elongated shape and long dendrites occur (Fig. 2d). A network of varicose fibers is present throughout the amygdala and the anterior commissure.

3.1.1.2. Diencephalon. In the neuropil of the anterior preoptic nucleus, many fibers, some with varicosities, are present. In the nucleus habenularis ventralis, numerous small, weakly stained cell bodies occur. The caudal part of the suprachiasmatic nucleus contains a few round perikarya, with a diameter of ca. 13 μm. They have a thick, short dendrite and the long process runs towards the ventricle, passing through the ependymal layer to contact the cerebrospinal fluid (CSF; Fig. 2e). In the ventromedial thalamic nucleus, a few small, positive perikarya occur, occupying an area that extends into a medial direction toward the third ventricle. Their primary and secondary dendrites are moderately immunoreactive. In the anterior thalamic nucleus, a few small, weakly stained perikarya were encountered. A few small cell bodies are present in the ventral hypothalamic nucleus with many varicose fibers running in different directions. In the paraventricular organ, some small perikarya are present, some of which extend a dendrite to the CSF (Fig. 2f). Laterally and medially from this organ, many fibers run near the third ventricle. In the posterior tubercle, a few small perikarya were observed. In this area, many fibers run near the ventricle and laterally to the posterior tubercle, some of them with varicosities. In both the ventral and medial part of the magnocellular

nucleus, some round cell bodies with moderate diameters (ca. 13 μm) were found (Fig. 2g). They send their axons in a tract toward the median eminence (Fig. 2h). The median eminence shows strong CRF-immunopositivity in both the internal and external zones. The external zone is studded with heavily stained axon terminals (Fig. 2i).

3.1.1.3. Pituitary gland. For the most part, the neural lobe of the pituitary gland is completely devoid of CRF-positive fibers. Only in a few paraffin sections come the CRF-immunoreactive fibers observed. They possess varicosities and occur mostly in the periphery of the lobe (Fig. 2j). In the intermediate and distal lobe of the pituitary gland, no CRF-positivity was seen.

3.1.1.4. Mesencephalon. The Edinger–Westphal nucleus reveals some positive fibers, which possess varicosities (Fig. 3a). However, no cell bodies were found. Numerous piriform cells and varicose fibers are present in the layers of the optic tectum (Figs. 3b, c). Many varicose fibers occur in the posterior commissure and in the tegmentum. In the anteroventral tegmental nucleus, some heavily stained cell bodies reveal a long dendrite running in the ventral direction (Fig. 3d). Many varicose fibers are present throughout the nucleus (Fig. 3d, inset). The torus semicircularis shows a few varicose fibers. The rare cell bodies in the posteroventral tegmental nucleus are small, and have a piriform shape and a short, thick dendrite.

3.1.1.5. Rhombencephalon. Some small, heavily stained cell bodies surrounded by fibers are present in the nucleus motorius nervi trigemini (Fig. 3e). In the locus coeruleus, some small perikarya were observed, with fibers running laterally (Fig. 3f). Also, the ventral part of the cerebellum shows some CRF-positive fibers.

3.1.2. UCN1

3.1.2.1. Telencephalon. Some UCN1-positive fibers were observed in the medial olfactory tract, the internal granule cell layer of the olfactory bulb, the dorsal pallium, the striatum, the nucleus accumbens, and in the diagonal band of Broca. In the medial septum, UCN1-positive fibers with small, beaded varicosities occur (Fig. 4a, inset). Furthermore, fibers showing some varicosities are present throughout the neuropil of the pars lateralis of the amygdala (Fig. 4b, inset) and the anterior commissure.

3.1.2.2. Diencephalon. In the neuropil of the anterior preoptic nucleus, long fibers with many varicosities are present. A small number (1–3) of cell bodies and some scattered fibers were encountered lateral to the suprachiasmatic nucleus. Rarely, fibers occur in the anterior, central, and posterior thalamic nucleus. In the posterior tubercle, several fibers run ventral to the posterior commissure, towards the optic recess. Cell bodies also occur in the paired magnocellular nucleus of the hypothalamus in both the ventral (Fig. 4c) and medial part (Fig. 4d) of the nucleus. Some neurons send processes toward the third ventricle, which may contact the CSF (Figs. 4c, d). In each nucleus, about 20 to 30 perikarya are strongly immunopositive, as are their axons, which can be followed into a ventrolateral direction, running towards the median eminence of the hypothalamus (Fig. 4e). The median eminence shows two UCN1-positive regions, an external zone with neurohemal axon terminals contacting the hypothalamo-hypophyseal portal system (Fig. 4f) and an internal zone through which numerous fibers pass to the pituitary neural lobe (Fig. 4g).

3.1.2.3. Pituitary gland. Throughout the neural lobe of the pituitary gland, numerous fibers are intensely UCN1-immunopositive and reveal numerous, large varicosities (Fig. 4h, inset). No UCN1-positivity was observed in the intermediate or distal lobe of the gland.

3.1.2.4. Mesencephalon. The Edinger–Westphal nucleus contains numerous UCN1-positive neurons. They are moderately sized (ca. 13 μm in diameter) and mostly piriform, showing primary, secondary, and sometimes tertiary dendrites (Fig. 5a). Some neurons are fusiform, with primary and sometimes secondary dendrites (Fig. 5b). The Edinger–Westphal nucleus also contains many UCN1-positive fibers. Some fibers are also present in the tegmentum mesencephali, in the tectum mesencephali and in the torus semicircularis. In the caudal part of the mesencephalon, in the nucleus posteroventralis tegmenti, some small, moderately stained cell bodies were observed, very close to the border of the cerebral aqueduct. The neuropil of the nucleus contains many fibers, whereas a few fibers appear in the neuropil of the interpeduncular nucleus.

3.1.2.5. Rhombencephalon. Some cell bodies are located in the nucleus motorius nervi trigemini. They are large (ca. 15 μm in diameter), multipolar, and rather weakly stained (Fig. 5c). The nucleus motorius of the facial and glossopharyngeal nerves shows several weakly stained cell bodies while sparse fibers run in the surroundings of the nucleus. Some lightly stained cells occur in the central gray. Small cell bodies are present in low numbers lateral to the nucleus reticularis medius. Furthermore, many varicose fibers occur in the cochlear nucleus (Fig. 5d, inset). In the nucleus motorius nervi vagi, some cell bodies were encountered, and laterally and medially to the solitary tract, a few fibers were seen.

3.2. Immuno-electron microscopy of the X. laevis pituitary neural lobe

To identify neurohemal axon terminals containing UCN1 and CRF, the neural lobe of the pituitary gland was investigated by immuno-electron microscopy. Neurointermediate lobes were prepared by HPF and cryosubstitution [8].

3.2.1. UCN1

At the ultrastructural level, the neural lobe shows numerous neurohemal axon terminals, situated near small blood vessels and capillaries (Fig. 6a). Two types of terminal were distinguished. The first type (A) contains large (mean diameter about 145 nm), round, and moderately

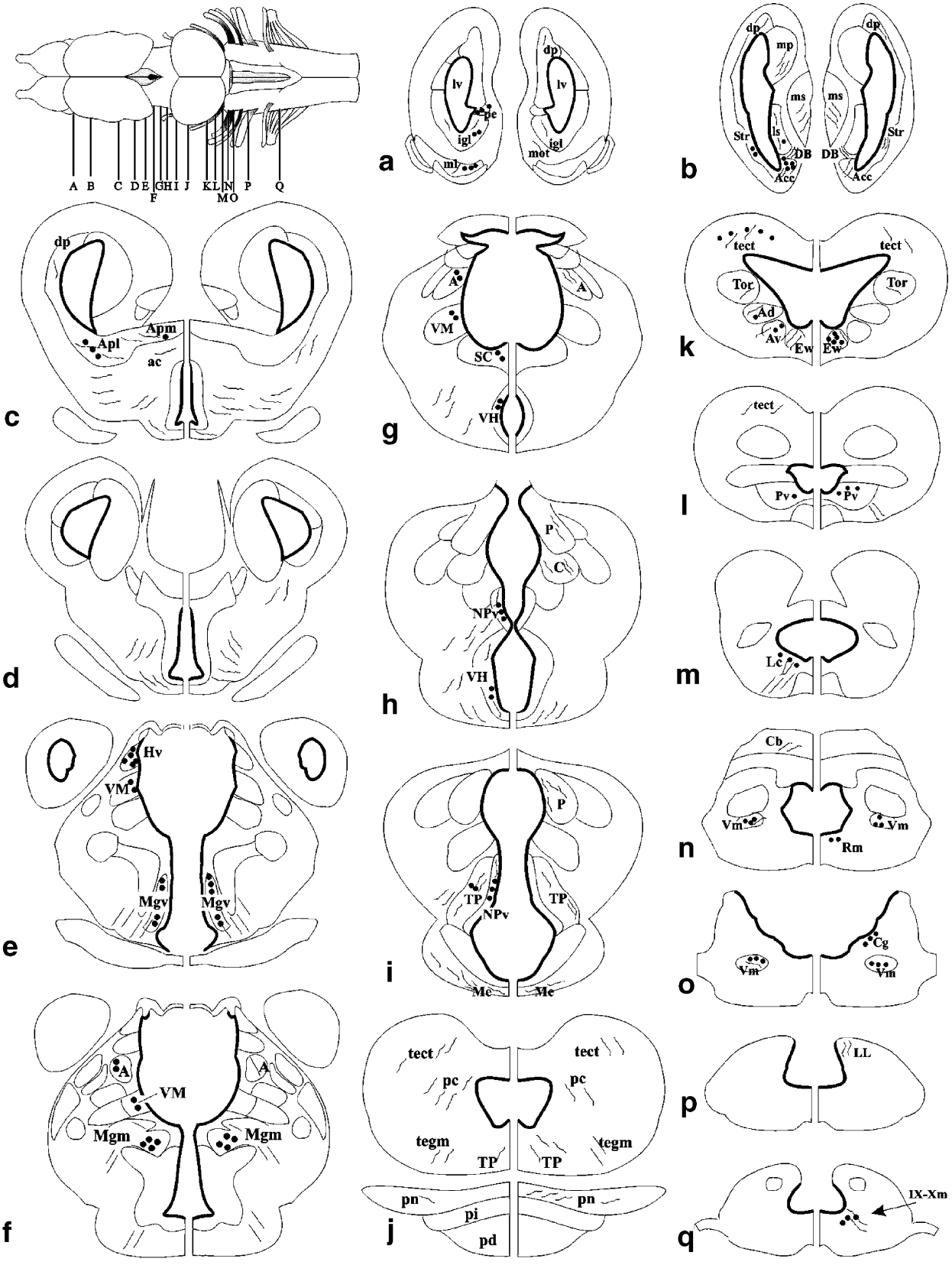

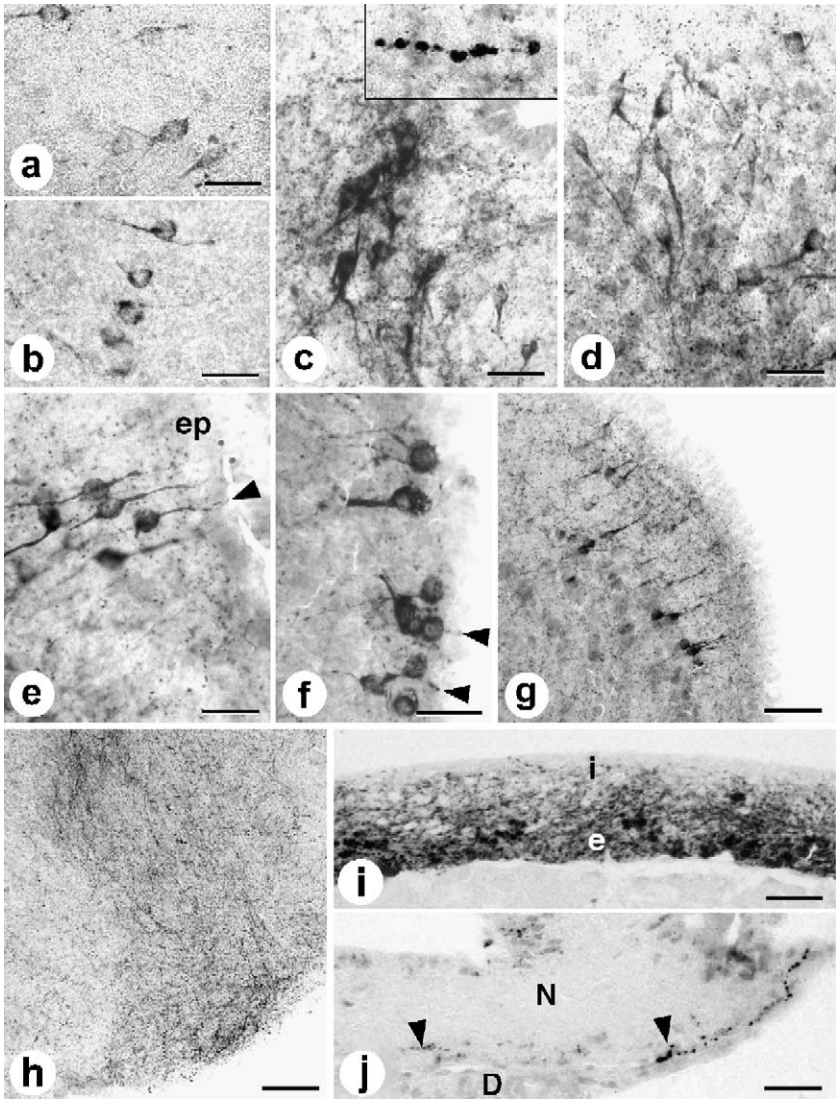

Fig. 2. Transverse sections at levels a–j (see Fig. 1) of the brain and pituitary gland of *X. laevis*, showing CRF-immunoreactive cell bodies and fibers. (a) Mitral cell layer. (b) Post-olfactory eminence. (c) Nucleus accumbens, with varicose fiber (inset). (d) Amygdala pars lateralis. (e) Suprachiasmatic nucleus, with arrowhead indicating dendrite contacting the CSF. ep, Ependymal cell layer. (f) Nucleus of the paraventricular organ, with dendrites contacting CSF (arrowheads). (g) Medial part of magnocellular nucleus. (h) Fiber tract running from the magnocellular nucleus to the median eminence. (i) Median eminence, with internal (i) and external (e) zone. (j) Neural lobe (N) and distal lobe (D) of the pituitary gland, with arrowheads indicating neurohemal axons. Scale bar a–f, i = 20 μm, g, h, j = 50 μm.

electron-dense granules, while the second type (B) is characterized by smaller, highly electron-dense granules. In contrast to type A, these terminals reveal ellipsoid or pleomorph granules with a mean long diameter of ca. 140 nm and a mean short diameter of ca. 100 nm (Fig. 6b). Immunogold particles indicating the presence of UCN1 occur over secretory granules in both terminal types (Figs. 6c, d). No appreciable numbers of gold particles were seen

Fig. 1. Top left: schematic dorsal view of the brain of *X. laevis*, with letters a–q indicating the levels of transverse sections (a–q) used in the study of CRF (on the left) and UCN1 (on the right) distribution. Immunoreactive cell bodies are indicated by black dots and immunoreactive main axon tracts by lines. A, anterior thalamic nucleus; ac, anterior commissure; Acc, nucleus accumbens; Ad, anterodorsal tegmental nucleus; Apl, amygdala, pars lateralis; Apm, amygdala, pars medialis; Av, anteroventral tegmental nucleus; Cb, cerebellum; DB, diagonal band of Broca; dp, dorsal pallium; EW, Edinger–Westphal nucleus; Hv, nucleus habenularis ventralis; igl, internal granule cells of the olfactory bulb; Lc, locus coeruleus; ls, lateral septum; lv, lateral ventricle; me, median eminence of the hypothalamus; Mgm, medial part of the magnocellular nucleus; Mgv, ventral part of the magnocellular nucleus; ml, mitral cell layer of the olfactory bulb; mot, medial olfactory tract; mp, medial pallium; ms, medial septum; NPv, nucleus of the paraventricular organ; nIX, nucleus motorius of the glossopharyngeus (glp) nerve; P, posterior thalamic nucleus; pc, posterior commissure; pd, pituitary gland, pars distalis; pe, post-olfactory eminence; pi, pituitary gland, pars intermedia; pn, pituitary gland, pars nervosa; Rm, nucleus reticularis medius; SC, suprachiasmatic nucleus; Str, striatum; tect, mesencephalic tectum; tegm, mesencephalic tegmentum; Tor, torus semicircularis; TP, posterior tubercle; VH, ventral hypothalamic nucleus; VM, ventromedial thalamic nucleus; Vm, nucleus motorius nervi trigemini; Xm, nucleus motorius nervi vagi.

outside the granules or in other neural lobe elements such as pituicytes, endothelium cells, or fibroblasts, or in melanotrope cells in the intermediate lobe (not shown).

3.2.2. CRF

At the ultrastructural level, in the neural lobe, neither A-type nor B-type terminals showed any appreciable amount of immunogold staining that would indicate the presence of CRF-immunoreactivity. Also, other elements of the neural lobe and the intermediate lobe were found to be immunonegative. Apparently, the CRF fibers seen at the light microscopic level in the neural lobe are too scarce to be identified by electron microscopy.

3.3. In vitro superfusion of X. laevis melanotrope cells

A superfusion study was conducted to test if UCN1 can stimulate αMSH release from dissociated melanotrope cells cultured in vitro. Exposure to UCN1 produced a clear dose-dependent stimulation of radiolabeled peptides release (Fig. 7). At a concentration of 10^{-10} M, UCN1 had no effect on the release of αMSH. At a concentration of 10^{-9} M UCN1, an increase of 15% in secretion took place, at 10^{-8} M and at 10^{-7} M, secretion was stimulated by more than 50%.

4. Discussion

4.1. CRF and UCN1 compared

In previous studies performed in amphibians [9,12,24,47], including *X. laevis* [45], CRF-positive perikarya in the CNS did not appear to be numerous, and seemed largely restricted to the preoptic area including the magnocellular nucleus. In these studies, CRF-positive axons were mainly seen in the external part of the median eminence and in some cases in the pituitary neural lobe [35,45]. By contrast, the present study on *X. laevis* reveals large numbers of CRF-immunopositive neurons and fibers in various parts of the brain, i.e., in the telencephalon, diencephalon, mesencephalon, and rhombencephalon. Our findings are in agreement with a recent report by Yao and colleagues [52] in juvenile *X. laevis*. In the hypothalamo-hypophyseal system, CRF is present in the magnocellular nucleus and in the external zone of the median eminence. By contrast to earlier studies, we found that CRF-positive fibers were scarce in the neural lobe of the pituitary gland and could only be detected at the light microscopic level. The explanation for the difference between this distribution and that found in earlier studies may be our use of a highly specific, affinity-purified anti-*Xenopus*-CRF serum, while in the other studies, an anti-mammalian CRF serum (also unpurified) was applied. On the basis of the present data, we conclude that CRF is widespread in the *X. laevis* brain, and thus could play a role in behavioral and autonomic responses to stress (by analogy to CRF in mammals). Our data also support the view that CRF in *X. laevis* acts as a neurohormone, being released from the external zone of the median eminence to stimulate hormone secretion by the anterior pituitary. The paucity of CRF-positive fibers in the neural lobe indicates that neurohormonal release from this part of the pituitary to control the melanotrope cells in the intermediate lobe is possible but likely to be rather unimportant, at least in a quantitative respect.

This study represents the first demonstration of UCN1 in the brain and pituitary gland of *X. laevis*. The distribution is clearly distinct from that of CRF. Both peptides are present in both the ventral and medial part of the magnocellular nucleus and in the nucleus motorius nervi trigemini, and various brain centers contain both UCN1- and CRF-ir fibers (amygdala, medial septum, nucleus accumbens, neuropil of the anterior preoptic nucleus, posterior tubercle, Edinger–Westphal nucleus and tectum). However, UCN1 also occurs in perikarya of the Edinger–Westphal nucleus, central gray, nucleus reticularis medius, nucleus motorius nervi facialis, and nucleus motorius nervi vagi where CRF-ir was not observed. Similarly, UCN1-ir, but not CRF-ir fibers run in the medial olfactory tract, central and anterior thalamic

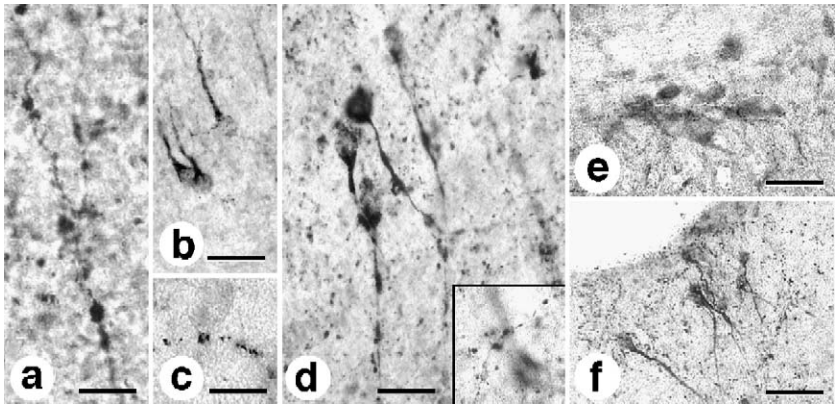

Fig. 3. Transverse sections at levels K–Q of the brain of *X. laevis*, showing CRF-immunoreactive cell bodies and fibers. (a) Varicose fibers in Edinger–Westphal nucleus. (b) Tectum mesencephali, cell bodies. (c) Tectum mesencephali, fibers. (d) Anterior tegmental nucleus, with varicose fiber in inset. (e) Nucleus motorius nervi trigemini. (f) Locus coeruleus. Scale bar a, c = 10 μm, b, d–f = 20 μm.

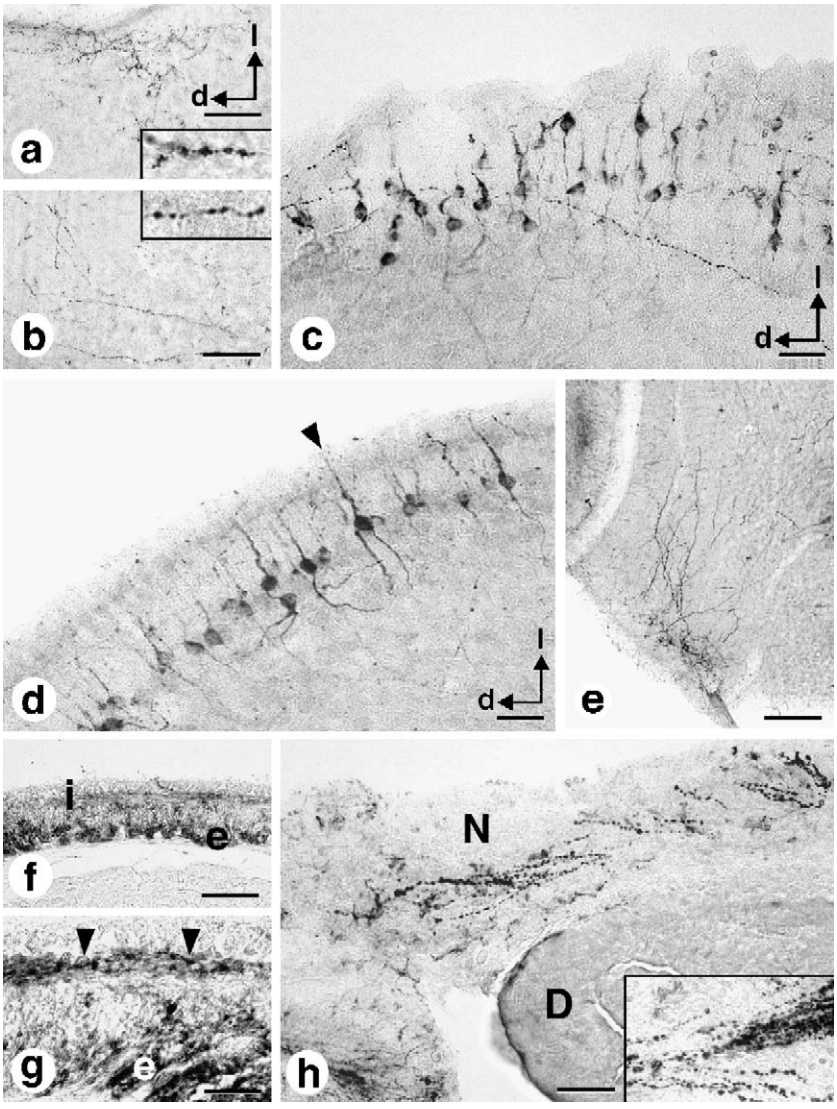

Fig. 4. Transverse sections from level A to level J of the brain and pituitary gland of *X. laevis*, presenting UCN1-immunoreactive cell bodies and fibers. (a) Medial septum. Inset: varicose fiber. (b) Amygdala pars lateralis. Inset: varicose fiber. (c) Ventral part of the magnocellular nucleus with arrowhead indicating dendrite contacting the CSF. (d) Medial part of the magnocellular nucleus. (e) Fiber tract running from the magnocellular nucleus to the median eminence. (f) Median eminence, with internal (i) and external (e) zone. (g) UCN1-positive fibers (arrowheads) running in the internal zone of the median eminence on their way to the neural lobe. (h) Neural lobe of the pituitary gland (N) with neurohemal axon terminals, shown in detail in inset. D, distal lobe. In a, b, and c, dorsal is not on top and orientation of dorsal (d)–lateral (l) has been indicated. Scale bar a–e, g = 20 μm, f = 50 μm, h = 10 μm.

nucleus, and nucleus posteroventralis tegmenti. Thus, the partial overlap in the distributions of UCN1 and CRF indicates that these two members of the CRF family could have some related, but also other unique neurotransmitters/neuromodulator and hypophysiotropic functions.

In amphibians, UCN1-ir has been described by us before, viz., in the frog *R. esculenta* [18]. However, the distribution of UCN1 in *X. laevis* shows clear differences with that in *R. esculenta*. In contrast to *R. esculenta*, in the *X. laevis* brain, no UCN1 is present in the anterior preoptic area, ventromedial thalamic nucleus, and posterior tubercle. The largest differences were found in the neuroendocrine system. In *X. laevis*, both the external and internal layer of the median eminence and the pituitary neural lobe show many immunopositive fibers, whereas in *R. esculenta*, only the external layer of the median eminence is immunopositive. These differences between the two amphibians might be explained by differences in the structure and/or the dynamics of their UCN1 systems. Alternatively, the differences could be related to technical differences between the two studies, where *R. esculenta*, but not *X. laevis*, had been pre-treated with colchicine to block axonal UCN1 transport leading to accumulation of the peptide within neuronal cell bodies [18].

In any case, the presence of strong dot-like UCN1-immunostaining of the external zone of the median eminence in *X. laevis* suggests that UCN1 occurs in neurohemal axon terminals of this neurohemal organ. Thus, UCN1 could be released into the pituitary portal system to act as a neurohormone on the melanotrope cells in the

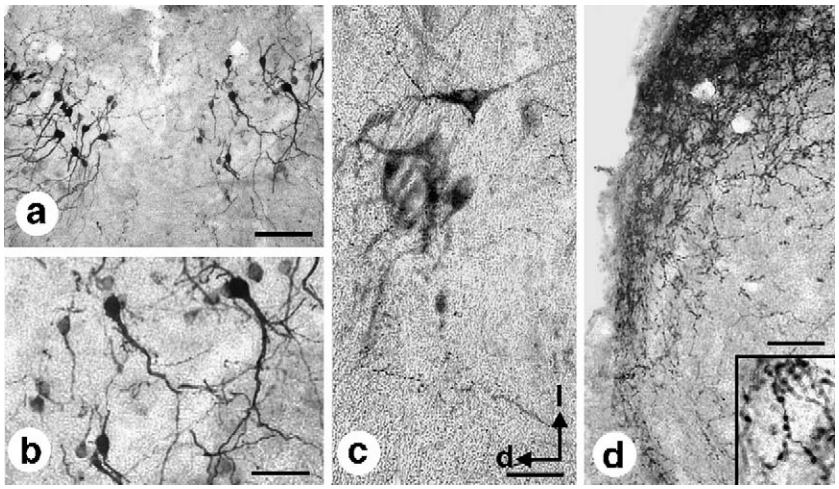

Fig. 5. Transverse sections at levels K–Q of the brain of *X. laevis*, with UCN1-immunoreactive cell bodies and fibers. (a) Edinger–Westphal nucleus. (b) Detail of (a), showing intricate dendritic ramifications. (c) Nucleus motorius nervi trigemini. (d) Cochlear nucleus, with varicose fiber in inset. In c, dorsal is not on top, and orientation of dorsal (d)–lateral (l) has been indicated. Scale bar a = 50 μm, b = 25 μm, c = 10 μm, d = 20 μm.

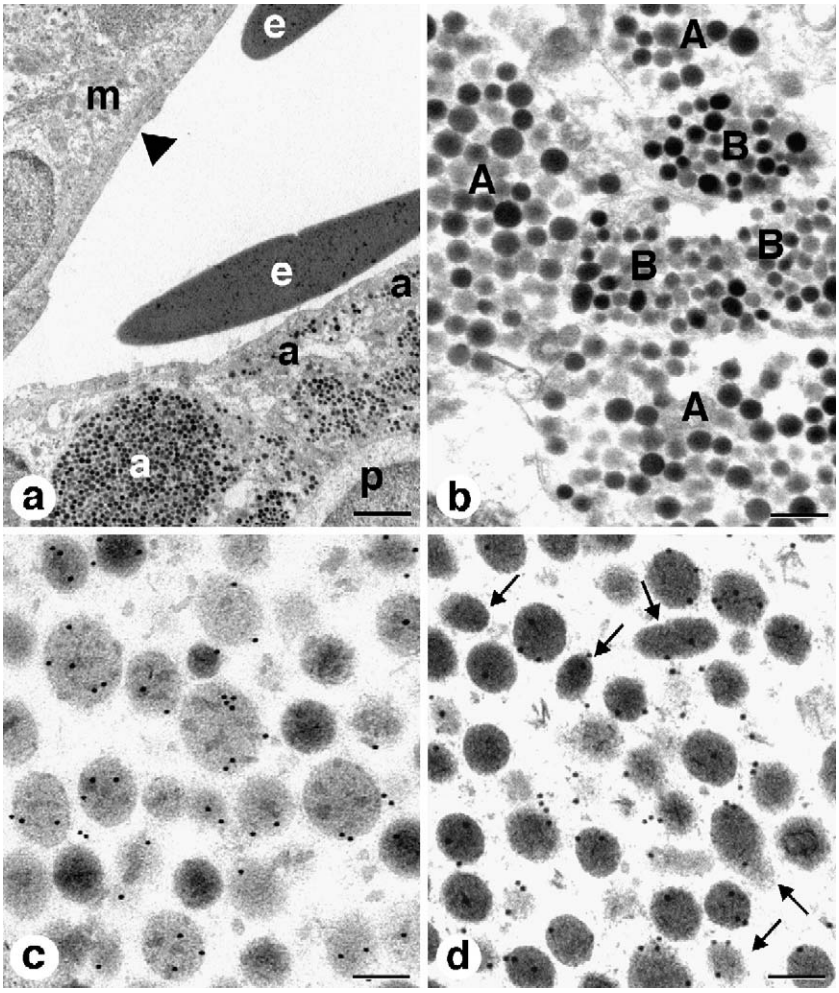

Fig. 6. Electron micrographs of (a) neurohemal axon terminals (a) in the pituitary neural lobe near blood vessel contacting melanotrope cell (m) in intermediate lobe. e, erythrocyte, p, pituicyte; arrowhead indicates endothelial cell lining vessel, (b) type A and type B terminals filled with secretory granules, (c) detail of type A axon terminals with large, moderately electron-dense granules immunoreactive (gold particles) to UCN1, (d) detail of type B axon terminals with many flat and pleomorph (arrows), mostly electron-dense granules immunoreactive (gold particles) to UCN1. Scale bar a = 1 μm, b = 300 nm, c, d = 200 nm.

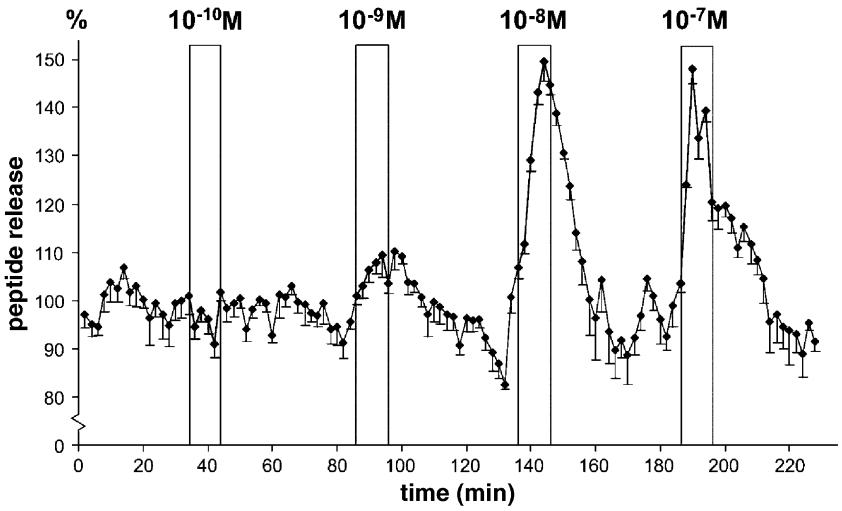

Fig. 7. Effect of different concentrations of *X. laevis* UCN1 (10^{-10} to 10^{-7} M) on the release of radiolabeled peptides (mainly αMSH; see [31]) from dissociated melanotrope cells superfused in vitro. Vertical grayed bars indicate 10-min fractions during which UCN1 was given. Secretion is expressed as a percentage of the control secretion level, which was set at 100% ($n = 4$).

intermediate lobe, and possibly also the corticotrope cells in the pars distalis [23].

4.2. UCN1 is released as a neurohormone from the pituitary neural lobe

Using light immunocytochemistry, we show the presence of UCN1-ir in the hypothalamo-neurohypophyseal system (HNS) of *X. laevis*. The light microscope data strongly indicate that a subpopulation of neurons in the magnocellular nucleus produce and transport UCN1 via axons toward the external zone of the median eminence, and via the internal zone of the eminence toward the neural lobe of the pituitary gland. The magnocellular nucleus of amphibians is considered to be homologous with the mammalian supraoptic and paraventricular nuclei [39]. In rat, both nuclei contain UCN1 [17,22] and UCN1 was also demonstrated at the light microscope level in fibers in the rat posterior pituitary [22]. The present study is the first to reveal the presence of UCN1 in the HNS of a non-mammalian vertebrate, highlighting the neuroendocrine importance of this evolutionarily conserved peptide.

To study the pituitary gland of *X. laevis* at the ultrastructural level, we applied the HPF technique, which yields excellent ultrastructural preservation of the *X. laevis* brain and pituitary gland, with maintenance of strong antigenicities for a variety of peptides and proteins [49]. Secretory granules appear perfectly preserved, not only as to their delineation, showing clear and straight bounding membranes, but also with regard to the different electron-densities of their contents, enabling the distinction between type A and type B neurohemal axon terminals in the neural lobe of the pituitary gland. Thanks to this technique, we demonstrate at the ultrastructural level that UCN1 occurs in the neural lobe within secretory granules in neurohemal axon terminals, indicating a neurohormonal role of UCN1. UCN1 is present in both type A and type B neurohemal axon terminals. This suggests that UCN1 is produced by at least two different neuron populations in the magnocellular nucleus. Recently, we showed that secretory granules in the type A neurohemal terminals in the *X. laevis* neural pituitary lobe contain the amphibian diuretic neurohormone mesotocin ([50]; L.C. Wang, unpublished results), which is known to be released from the neural lobe [25]. This indicates that these terminals release mesotocin together with UCN1, providing strong evidence that UCN1 is released from the amphibian neural lobe as a neurohormone.

Interestingly, type A but not type B terminals are immunopositive to mesotocin and to brain-derived neurotrophic factor (BDNF) ([50]; L.C. Wang, unpublished results), indicating that the two populations of UCN1-producing neurons in the magnocellular nucleus innervating the neural lobe do not only differ as to their capacity to produce mesotocin but also to produce BDNF.

4.3. UCN1 stimulates αMSH release

The functional role of UCN1 released from the *X. laevis* neural lobe is not known, but in view of the fact that the neural lobe is closely apposed to the intermediate lobe, it is likely that neurohormonally released UCN1 will readily reach the melanotrope cells to stimulate their secretory activity. The fact that our in vitro superfusion study shows that UCN1 is able to stimulate the release of αMSH from *X. laevis* melanotrope cells in a dose-dependent fashion supports this idea. This stimulation may be very effective, as even at a concentration as low as 10^{-8} M a clear stimulatory effect was noted. Because of the high affinity of UCN1 for the CRF_2 receptor (mammals: [44]; *X. laevis*: G.C. Boorse and R.J. Denver, unpublished results), the recent demonstration by RT-PCR of *X. laevis* CRF_2 mRNA [5–7] in the neurointermediate lobe of the *X. laevis* pituitary

(B.G. Jenks, unpublished results) is another strong indication that UCN1 released from the neural lobe can stimulate αMSH release by *X. laevis* melanotrope cells.

4.4. UCN1 and other messengers in the neural lobe

In amphibians, mesotocin has a diuretic action, most likely acting peripherally, on kidney, skin, and bladder [25,51]. This raises the question as to the functional significance of the coexistence in type A terminals of UCN1, controlling the nearby melanotrope cells, with mesotocin, acting on peripheral organs. Obviously, we cannot exclude the possibility that UCN1 released from the neural lobe (also) has peripheral actions [13,26], but it is noteworthy that not only UCN1 but also mesotocin has a stimulatory action on the release of αMSH from the *X. laevis* intermediate lobe (L.C. Wang and G.J.H. Corstens, unpublished results). This effect is in contrast with the situation in the frog *R. ridibunda*, where mesotocin does not affect αMSH release from the pituitary intermediate lobe [36]. Apparently, in *X. laevis*, both UCN1 and mesotocin can activate αMSH secretion in a neurohormonal way.

In addition to CRF, UCN1, and mesotocin, three other factors have been shown to be present in the neural pituitary lobe of *X. laevis*, viz., vasotocin, brain-derived neurotrophic factor (BDNF) and TRH ([5,46,50], L.C. Wang, unpublished results). Each of these factors stimulates αMSH release from *X. laevis* melanotrope cells in vitro ([20,46]; L.C. Wang, B.G. Jenks, unpublished results). This strongly suggests that the neural lobe is an important site of neurohormonal control of the melanotrope cells, being responsible for the neurohormonal release of multiple stimulatory messengers. This highlights the functional significance of the close anatomical association between the neural and intermediate lobe in the pituitary gland.

As retrograde tracing of the neural lobe shows only labeling of the magnocellular nucleus [42,50], all messengers present in the neural lobe, viz., CRF, UCN1, mesotocin, vasotocin, BDNF, and TRH, must be produced in the magnocellular nucleus. Detailed colocalization studies will have to further elucidate possible coexistence of these factors in various subpopulations of magnocellular neurons and their neurohemal axon terminal types.

In the frogs, *R. ridibunda* and *Rana catesbeiana*, mesotocin-containing axons in the pituitary neural lobe also contain thyrotropin-releasing hormone (TRH) [21,32], which is known to stimulate αMSH release from *R. ridibunda* [10,11,43]. Therefore, the important role of the neural lobe in the control of melanotrope cells may apply to amphibians in general.

4.5. Control of neurohormonal UCN1 secretion

The question arises as to the nature of the stimuli that activate magnocellular neurons to release UCN1 and mesotocin from the neural lobe axon terminals into the circulation. In mammals, UCN1 may be an important component of the stress response mechanism [18,19,44]. Hyperosmotic stress is known to activate *c-fos* expression in the *X. laevis* magnocellular nucleus [41]. Whether stressors like osmotic stress would activate UCN1 mRNA expression in this nucleus and stimulate the release of UCN1 (and of other messengers) from the neural pituitary lobe, awaits investigation, as is the possibility that UCN1 production and release is under the control of the background adaptation condition.

4.6. Conclusions

Because of its distribution pattern, UCN1 may have widespread local actions in the *X. laevis* brain. Its presence in the neuroendocrine system strongly indicates that it is also a neurohormone. We provide evidence that UCN1 released from the neural lobe may control the secretory activity of the melanotrope cells in the adjacent intermediate lobe. In mammals, UCN1 has, in addition to its central actions, various actions on peripheral organs like the heart and gut. Therefore, the possibility that UCN1, released from the neural lobe into the systemic circulation, also acts on peripheral targets deserves investigation.

Acknowledgments

The authors are very grateful to Jean Rivier and Wylie W. Vale of the Salk Institute, La Jolla, for supplying the synthetic *X. laevis* CRF and the rat UCN1 antiserum, to Will J.A.J. Smeets of the Vrije Universiteit Amsterdam for anatomical advise, to Frouwke J. Kuijpers-Kwant and Kari H.A. Meijer for technical assistance, and to Ron J.C. Engels for animal care. Partial support for this project was provided by a grant from National Science Foundation of the USA IBN 0235401 to R.J.D., and a grant from the Netherlands Organization of Scientific Research.

References

[1] K. Asaba, S. Makino, K. Hashimoto, Effect of urocortin on ACTH secretion from rat anterior pituitary in vitro and in vivo: comparison with corticotropin-releasing hormone, Brain Res. 806 (1998) 95–103.
[2] J.C. Bittencourt, J. Vaughan, C. Arias, R.A. Rissman, W.W. Vale, P.E. Sawchenko, Urocortin expression in rat brain: evidence against a pervasive relationship of urocortin-containing projections with targets bearing type 2 CRF receptors, J. Comp. Neurol. 415 (1999) 285–312.
[3] G.C. Boorse, R.J. Denver, Expression and hypophysiotropic actions of corticotropin-releasing factor in *Xenopus laevis*, Gen. Comp. Endocrinol. 137 (2004) 272–282.
[4] S.C. Coste, R.F. Quintos, M.P. Stenzel-Poore, Corticotropin-releasing hormone-related peptides and receptors: emergent regulators of cardiovascular adaptations to stress, Trends Cardiovasc. Med. 12 (2002) 176–182.
[5] F.M. Dautzenberg, K. Dietrich, M.R. Palchaudhuri, J. Spiess, Identification of two corticotropin-releasing factor receptors from

Xenopus laevis with high ligand selectivity: unusual pharmacology of the type 1 receptor, J. Neurochem. 69 (1997) 1640–1649.
[6] F.M. Dautzenberg, S. Wille, R. Lohmann, J. Spiess, Mapping of the ligand-selective domain of the *Xenopus laevis* corticotropin-releasing factor receptor 1: implications for the ligand-binding site, Proc. Natl. Acad. Sci. U. S. A. 95 (1998) 4941–4946.
[7] F.M. Dautzenberg, J. Higelin, O. Brauns, B. Butscha, R.L. Hauger, Five amino acids of the *Xenopus laevis* CRF (corticotropin-releasing factor) type 2 receptor mediate differential binding of CRF ligands in comparison with its human counterpart, Mol. Pharmacol. 61 (2002) 1132–1139.
[8] C.J. Donaldson, S.W. Sutton, M.H. Corrigan, K.A. Lewis, J.E. Rivier, J.M. Vaughan, W.W. Vale, Cloning and characterization of human urocortin, Endocrinology 137 (1996) 2167–2170.
[9] A. Fasolo, C. Andreone, F. Vandesande, Immunohistochemical localization of corticotropin-releasing factor (CRF)-like immunoreactivity in the hypothalamus of the newt, *Triturus cristatus*, Neurosci. Lett. 49 (1984) 135–142.
[10] L. Galas, M. Lamacz, M. Garnier, E.W. Roubos, M.C. Tonon, H. Vaudry, Involvement of extracellular and intracellular calcium sources in TRH-induced alpha-MSH secretion from frog melanotrope cells, Mol. Cell. Endocrinol. 138 (1998) 25–39.
[11] L. Galas, M. Lamacz, M. Garnier, E.W. Roubos, M.C. Tonon, H. Vaudry, Involvement of protein kinase C and protein tyrosine kinase in thyrotropin-releasing hormone-induced stimulation of alpha-melanocyte-stimulating hormone secretion in frog melanotrope cells, Endocrinology 140 (1999) 3264–3272.
[12] G.C. Gonzalez, K. Lederis, Sauvagine-like and corticotropin-releasing factor-like immunoreactivity in the brain of the bullfrog (*Rana catesbeiana*), Cell Tissue Res. 253 (1988) 29–37.
[13] Y. Huang, X.Q. Yao, C.W. Lau, Y.C. Chan, S.Y. Tsang, F.L. Chan, Urocortin and cardiovascular protection, Acta Pharmacol. Sin. 25 (2004) 257–265.
[14] B.G. Jenks, H.J. Leenders, G.J.M. Martens, E.W. Roubos, Adaptation physiology: the functioning of pituitary melanotrope cells during background adaptation of the amphibian *Xenopus laevis*, Zool. Sci. 10 (1993) 1–11.
[15] B.G. Jenks, E.W. Roubos, W.J.J.M. Scheenen, Ca^{2+} oscillations in melanotropes of *Xenopus laevis*: their generation, propagation and function, Gen. Comp. Endocrinol. 131 (2003) 210–219.
[16] T. Kozicz, Neurons colocalizing urocortin and cocaine and amphetamine-regulated transcript immunoreactivities are induced by acute lipopolysaccharide stress in the Edinger–Westphal nucleus in the rat, Neuroscience 116 (2003) 315–320.
[17] T. Kozicz, H. Yanaihara, A. Arimura, Distribution of urocortin-like immunoreactivity in the central nervous system of the rat, J. Comp. Neurol. 391 (1998) 1–10.
[18] T. Kozicz, A. Arimura, J.L. Maderdrut, G. Lazar, Distribution of urocortin-like immunoreactivity in the central nervous system of the frog *Rana esculenta*, J. Comp. Neurol. 453 (2002) 185–198.
[19] T. Kozicz, A. Korosi, C. Korsman, D.T.W.M. Tilburg-Ouwens, L. Groenink, J.G. Veening, J. van der Gugten, E.W. Roubos, B. Olivier, Urocortin expression in the Edinger–Westphal nucleus is down-regulated in transgenic mice over-expressing neuronal corticotropin-releasing factor, Neuroscience 123 (2004) 589–594.
[20] B.M.R. Kramer, P.M.J.M. Cruijsen, D.T.W.M. Ouwens, M.W. Coolen, G.J.M. Martens, E.W. Roubos, B.G. Jenks, Evidence that brain-derived neurotrophic factor acts as an autocrine factor on pituitary melanotrope cells of *Xenopus laevis*, Endocrinology 143 (2002) 1337–1345.
[21] M. Lamacz, C. Hindelang, M.C. Tonon, H. Vaudry, M.E. Stoeckel, Three distinct thyrotropin-releasing hormone-immunoreactive axonal systems project in the median eminence–pituitary complex of the frog *Rana ridibunda*. Immunocytochemical evidence for co-localization of thyrotropin-releasing hormone and mesotocin in fibres innervating pars intermedia cells, Neuroscience 32 (1989) 451–462.
[22] S.M. Morin, N. Ling, X.J. Liu, S.D. Kahl, D.R. Gehlert, Differential distribution of urocortin- and corticotropin-releasing factor-like immunoreactivities in the rat brain, Neuroscience 92 (1999) 281–291.
[23] H. Ohata, K. Suzuki, Y. Oki, T. Shibasaki, Urocortin in the ventromedial hypothalamic nucleus acts as an inhibitor of feeding behavior in rats, Brain Res. 861 (2000) 1–7.
[24] M. Olivereau, F. Vandesande, E. Boucique, F. Ollevier, J.M. Olivereau, Immunocytochemical localization and spatial relation to the adenohypophysis of a somatostatin-like and a corticotropin-releasing factor-like peptide in the brain of four amphibian species, Cell Tissue Res. 247 (1987) 317–324.
[25] P.K. Pang, W.H. Sawyer, Renal and vascular responses of the bullfrog (*Rana catesbeiana*) to mesotocin, Am. J. Physiol. 235 (1978) 151–155.
[26] D.G. Parkes, R.S. Weisinger, C.N. May, Cardiovascular actions of CRH and urocortin: an update, Peptides 22 (2001) 821–827.
[27] E.W. Roubos, Background adaptation by *Xenopus laevis*: a model for studying neuronal information processing in the pituitary pars intermedia, Comp. Biochem. Physiol. 118 (1997) 533–550.
[28] E.W. Roubos, W.J.J.M. Scheenen, B.G. Jenks, Neuroendocrinology, from concepts and complexity to integration—The *Xenopus* pars intermedia, in: H.J.T. Goos, R.K. Rastogi, H. Vaudry, R. Pierantoni (Eds.), Perspective in Comparative Endocrinology: Unity and Diversity, Monduzzi Editore, Bologna, 2001, pp. 465–472.
[29] E.W. Roubos, W.J.J.M. Scheenen, P.M.J.M. Cruijsen, L.N. Cornelisse, H.J. Leenders, B.G. Jenks, New aspects of signal transduction in the *Xenopus laevis* melanotrope cell, Gen. Comp. Endocrinol. 126 (2002) 255–260.
[30] E.W. Roubos, W.J.J.M. Scheenen, B.G. Jenks, Neuronal, neurohormonal and autocrine control of *Xenopus* melanotrope cell activity, in: H. Vaudry et al. (Eds.), Trends in Comparative Endocrinology and Neurobiology, Ann. N.Y. Acad. Sci. (in press).
[31] W.J.J.M. Scheenen, H.G. Yntema, P.H. Willems, E.W. Roubos, J.R. Lieste, B.G. Jenks, Neuropeptide Y inhibits Ca^{2+} oscillations, cyclic AMP, and secretion in melanotrope cells of *Xenopus laevis* via a Y1 receptor, Peptides 16 (1995) 889–895.
[32] S. Shioda, Y. Nakai, C. Iwai, H. Sunayama, Co-existence of TRH with mesotocin in the same axon terminals of the bullfrog pars nervosa as revealed by double labeling immunocytochemistry, Neurosci. Lett. 98 (1989) 25–28.
[33] K.H. Skelton, M.J. Owens, C.B. Nemeroff, The neurobiology of urocortin, Regul. Pept. 93 (2000) 85–92.
[34] M.P. Stenzel-Poore, K.A. Heldwein, P. Stenzel, S. Lee, W.W. Vale, Characterization of the genomic corticotropin-releasing factor (CRF) gene from *Xenopus laevis*: two members of the CRF family exist in amphibians, Mol. Endocrinol. 6 (1992) 1716–1724.
[35] M.C. Tonon, A. Burlet, M. Lauber, P. Cuet, S. Jégou, L. Gouteux, N. Ling, H. Vaudry, Immunohistochemical localization and radioimmunoassay of corticotropin-releasing factor in the forebrain and hypophysis of the frog *Rana ridibunda*, Neuroendocrinology 40 (1985) 109–119.
[36] M.C. Tonon, P. Cuet, M. Lamacz, S. Jégou, J. Cote, L. Gateaux, N. Ling, G. Pelletier, H. Vaudry, Comparative effects of corticotropin-releasing factor, arginine vasopressin, and related neuropeptides on the secretion of ACTH and alpha-MSH by frog anterior pituitary cells and neurointermediate lobes in vitro, Gen. Comp. Endocrinol. 61 (1986) 438–445.
[37] Y. Tonosaki, P.M.J.M. Cruijsen, K. Nishiyama, H. Yaginuma, E.W. Roubos, Regulation of α-MSH release from the pituitary pars intermedia of *Xenopus laevis* in a cold environment, in: H.J.T. Goos, R.K. Rastogi, H. Vaudry, R. Pierantoni (Eds.), Perspective in Comparative Endocrinology: Unity and Diversity, Monduzzi Editore, Bologna, 2001, pp. 821–826.
[38] Y. Tonosaki, P.M.J.M. Cruijsen, K. Nishiyama, H. Yaginuma, E.W. Roubos, Low temperature stimulates α-MSH secretion and inhibits background adaptation in *Xenopus laevis*, J. Neuroendocrinol. 16 (2004) 894–905.

[39] R. Tuinhof, C. Artero, A. Fasolo, M.F. Franzoni, H.J. ten Donkelaar, P.G. Wismans, E.W. Roubos, Involvement of retinohypothalamic input, suprachiasmatic nucleus, magnocellular nucleus and locus coeruleus in control of melanotrope cells of *Xenopus laevis*: a retrograde and anterograde tracing study, Neuroscience 61 (1994) 411–420.

[40] A.V. Turnbull, C. Rivier, Corticotropin-releasing factor (CRF) and endocrine responses to stress: CRF receptors, binding protein, and related peptides, Proc. Soc. Exp. Biol. Med. 215 (1997) 1–10.

[41] R. Ubink, B.G. Jenks, E.W. Roubos, Physiologically induced Fos expression in the hypothalamo-hypophyseal system of *Xenopus laevis*, Neuroendocrinology 65 (1997) 413–422.

[42] R. Ubink, R. Tuinhof, E.W. Roubos, Identification of suprachiasmatic melanotrope-inhibiting neurons in *Xenopus laevis*: a confocal laser-scanning microscopy study, J. Comp. Neurol. 397 (1998) 60–68.

[43] H. Vaudry, M.C. Trochard, F. Leboulenger, R. Vaillant, Control of pituitary secretion of melanotropin in an anuran amphibian by thyrotropin releasing factor (TRH). Study in vitro, C. R. Acad. Sci., Hebd. Séances Acad. Sci. D 284 (1977) 961–965.

[44] J. Vaughan, C. Donaldson, J. Bittencourt, M.H. Perrin, K. Lewis, S. Sutton, R. Chan, A.V. Turnbull, D. Lovejoy, C. Rivier, Urocortin, a mammalian neuropeptide related to fish urotensin I and to corticotropin-releasing factor, Nature 378 (1995) 287–292.

[45] B.M.L. Verburg-van Kemenade, B.G. Jenks, P.M.J.M. Cruijsen, A. Dings, M.C. Tonon, H. Vaudry, Regulation of MSH release from the neurointermediate lobe of *Xenopus laevis* by CRF-like peptides, Peptides 8 (1987) 1093–1100.

[46] B.M.L. Verburg-van Kemenade, B.G. Jenks, T.J. Visser, M.C. Tonon, H. Vaudry, Assessment of TRH as a potential αMSH-release stimulating factor in *Xenopus laevis*, Peptides 8 (1987) 69–76.

[47] P. Verhaert, S. Marivoet, F. Vandesande, A. De Loof, Localization of CRF immunoreactivity in the central nervous system of three vertebrate and one insect species, Cell Tissue Res. 238 (1984) 49–53.

[48] C. Wang, M.A. Mullet, M.J. Glass, C.J. Billington, A.S. Levine, C.M. Kotz, Feeding inhibition by urocortin in the rat hypothalamic paraventricular nucleus, Am. J. Physiol., Regul. Integr. Comp. Physiol. 280 (2001) 473–480.

[49] L.C. Wang, H.K. Meijer, B.M. Humbel, B.G. Jenks, E.W. Roubos, Activity-dependent dynamics of coexisting brain-derived neurotrophic factor, pro-opiomelanocortin and alpha-melanophore-stimulating hormone in melanotrope cells of *Xenopus laevis*, J. Neuroendocrinol. 16 (2004) 19–25.

[50] L.C. Wang, M. Calle, E.W. Roubos, Brain-derived neurotrophic factor in the hypothalamo-hypophyseal system of *Xenopus laevis*, in: H. Vaudry et al. (Eds.), Trends in Comparative Endocrinology and Neurobiology, Ann. N.Y. Acad. Sci. (in press).

[51] M.R. Warburg, Hormonal effect on the osmotic, electrolyte and nitrogen balance in terrestrial Amphibia, Zool. Sci. 12 (1995) 1–11.

[52] M. Yao, N.J. Westphal, R.J. Denver, Distribution and stressor-induced activation of corticotrophin-releasing factor neurons in the CNS of *Xenopus laevis*, J. Neuroendocrinol. 16 (2004) 880–893.

[53] L. Zhao, C.J. Donaldson, G.W. Smith, W.W. Vale, The structures of the mouse and human urocortin genes (Ucn and UCN), Genomics 50 (1998) 23–33.